International Journal of Control and Automation
Vol. 8, No. 6 (2015), pp. 27-34
http://dx.doi.org/10.14257/ijca.2015.8.6.04

A Novel Reflective Fiber Optic Current Sensor and Error Characteristics in the Key Optical Components

Shen Tao[1, 2], Feng Yue[2], Dai Hailong[2], Hu Chao[2] and Wei Xinlao[1]

[1]*Key Laboratory of Engineering Dielectrics and Its Application, Ministry of Education , Harbin University of Science and Technology, 150080 Harbin, China*
[2]*School of Applied Sciences, Harbin University of Science and Technology, 150080 Harbin, China*
taoshenchina@163.com

Abstract

Fiber optical current sensors based on Faraday effect have a lot of advantages over conventional current sensors and have been studied extensively. To eliminate the vibration sensitivity, a light path of reflective fiber optic current sensor improved is proposed, which makes discharge of Sagnac effect with Sagnac effect itself and do not disturb Faraday Effect at all. The reliability of the system was simulated, then the polarization states for the key optical components of the lights spreading in the improved light path are analyzed with Jones matrix. The results shows that the output of the improved sensor is accordance with the actual case. A new solution for guarantee the term running of fiber-optic current transformer was provided, a feasible method for the practical use of Sagnac fiber-optic current sensor is provided.

Keywords: *Optical current sensor, error characteristics, Faraday effect, Jones matrix Sagnac effect*

1. Introduction

After the technological revolutions of the last few decades, with unimaginable technological advances in the area of information and communications technology, the electrical sector had turned into an anachronism using the technology of last century. Optical technology is an ideal candidate for this, without the safety requirements of conventional sensors. Current sensors (CS) always play a very important role in the electric power industry. In a long time and even up to now, current sensors for metering and protective relaying applications are almost conventional current sensors based on electromagnetic coupling method. Although conventional current sensor is well-developed and widely-accepted, it is very difficult for current sensors based on conventional technology to meet the demand of increasing current level. They are always heavy and expensive to obtain high insulation level which is necessary in high level power system. This difficulty stimulates some researchers to pursue novel approaches to measure current. As a consequence, the optical current sensor (OCS) emerged in 1970s. OCS based on optical fiber sensors are now being developed worldwide. In comparison with conventional transformers, fiber optical current sensors (FOCS) are compact and lightweight, easy to install, immune to electromagnetic noise, and they offer a wide measurement range and long distance signal transmission. To date, a number of FOCS have been shown to be feasible. They have good reliability and sensitivity, although the price is also high.

As it can be seen, substantial progress in optical current sensing field has been achieved during the last decades. However, the temperature stability and long-term reliability have been the obstacles which restrict the application of OCSs in electric power system. So, the research should be continued in-depth. This paper reports the novel FOCS

ISSN: 2005-4297 IJCA

based on the Faraday Magneto-Optic effect with a Sagnac loop interferometer's reflective type was designed, error characteristics in the key optical components was studied, including y-branch and 90o offset. It is expected to get practical application in power system.

2. Basic Principle

Most of optical current sensors are based on Faraday Effect, which is that the polarization direction is rotated by the magnetic field paralleling with the direction of the optical beams. When the optical path is closed, the rotation angle of the polarization plane is in proportion to the product of the Verdet constant of the sensing materials and the current generating the magnetic field. FOCS were categorized on whether the sensing head has been powered. It can be divided into active device and passive device. In this paper, the FOCS is passive device, the main working principle is Faraday magneto-optic effect [18].

The Faraday effect, used in some medium, is a magnetically induced circular birefringence. A beam of light flowing through a fiber with a magnetic field present will have its linear polarization state rotated through an angle $\Delta\varphi$, it is proportional to magnetic field intensity H, and the length of light path in magnetic field L [18].

$$\Delta\varphi = VHL \tag{1}$$

Where V is the Verdet constant. Figure 1 shows a schematic configuration of the Faraday rotation. When a light beam passes through a glass medium in a magnetic field, its polarization vector is rotated in proportion to the field. The Verdet constant V relates the line integral of the magnetic field H to the rotation of the polarization plane of a linearly polarized

For FOCS, a magnetic field will be built up round the current-carrying wire, satisfying Ampere's circuital law. Therefore, the rotation angle in the fiber:

$$\Delta\varphi = V\oint Hdl = NVI \tag{2}$$

Where N is the number of turns of sensing optical fiber ring, I is the current in optical fiber.

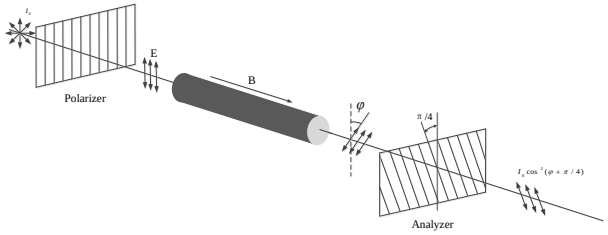

Figure 1. Faraday Rotation

3. Sensor Configuration

The external vibration is one of the most important limitations of Sagnac FOCS. The sensor exploits the Faraday effect in a fused silica fiber. An interrogation technique as known from closed-loop fiber gyroscopes, is used to recover the magneto-optic phase shift. The novel setup shown in Figure 2 allows one to use a standard y-branch integrated optics phase modulator of a fiber gyro, an external compensation coil of delay, rather than the piezoelectric birefringence modulator considered earlier.

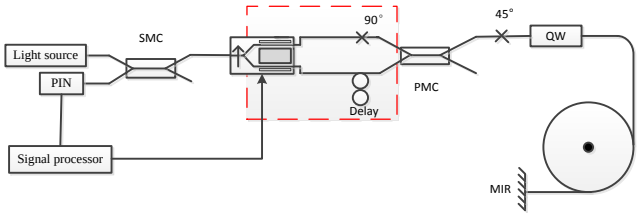

Figure 2. Fiber-Optic Current Sensor

Figure 3 is an improved proposed structure for external compensation coil of delay, it able to fully offset the impact on Sagnac effect because of the compensation coil and sensing coil feel the vibration factors also exactly the opposite. And compensation coil and sensing coil is wound in the same fiber, reducing the impact on the complexity of the FOCS.

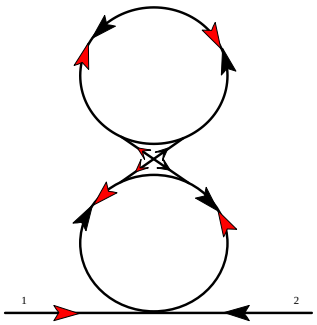

Figure 3. Structure of External Compensation Coil

4. Model Analysis

There are two assumptions in the establishment of open-loop model from the graph, one is medium without scattering and backscattering, anther is system is reciprocal.

Jones matrix of each device as follows in ideally:

The polarizer: $L_P = \begin{bmatrix} 1 & 1 \\ 1 & 1 \end{bmatrix}$

Fiber Coupler: $L_{MC} = \frac{1}{\sqrt{2}} \begin{bmatrix} 1 & 0 \\ 0 & 1 \end{bmatrix}$

45°splice: $L_{45} = \frac{1}{\sqrt{2}} \begin{bmatrix} 1 & 1 \\ -1 & 1 \end{bmatrix}$

90°splice: $L_{90} = \begin{bmatrix} 0 & -1 \\ 1 & 1 \end{bmatrix}$

1/4 wave plate: $L_{\lambda/4} = \frac{1}{\sqrt{2}} \begin{bmatrix} 1 & i \\ i & 1 \end{bmatrix}$

Faraday effect: $L_{fin} = \begin{bmatrix} \cos\theta & -\sin\theta \\ \sin\theta & \cos\theta \end{bmatrix}$ $L_{fout} = \begin{bmatrix} \cos\theta & \sin\theta \\ -\sin\theta & \cos\theta \end{bmatrix}$

A standard y-branch integrated-optics phase modulator of a fiber gyro was adopt of system, rather than the piezoelectric birefringence modulator considered earlier [21]. Piezoelectric modulators are mostly employed in combination with open-loop signal processing. It use of the push-pull working methods, that is the voltage was modulated with two waveguides of two waves propagating in opposite directions by the time difference.

L_1 and L_2 are set to $(t-\tau)$ and t moment's Jones matrix of Y waveguide above modulator arm, L_3 and L_4 are set to $(t-\tau)$ and t moment's Jones matrix of Y waveguide below modulator arm [22].

$$L_1 = \begin{bmatrix} e^{i\varphi(t-\tau)} & 0 \\ 0 & 1 \end{bmatrix} \quad L_2 = \begin{bmatrix} e^{i\varphi(t)} & 0 \\ 0 & 1 \end{bmatrix}$$

$$L_3 = \begin{bmatrix} e^{-i\varphi(t-\tau)} & 0 \\ 0 & 1 \end{bmatrix} \quad L_4 = \begin{bmatrix} e^{-i\varphi(t)} & 0 \\ 0 & 1 \end{bmatrix}$$

The dotted line in Figure 2 as a device, Jones matrix of pros and cons to each as:

$$L_{out} = (L_4 \cdot L_D + L_2 \cdot L_{90}) = \begin{bmatrix} e^{-i\varphi(t)} & -e^{i\varphi(t)} \\ 1 & 1 \end{bmatrix}$$

$$L_{in} = (L_{90} \cdot L_1 + L_D \cdot L_3) = \begin{bmatrix} e^{-i\varphi(t-\tau)} & -1 \\ e^{i\varphi(t-\tau)} & 1 \end{bmatrix}$$

Jones matrix with back through the optical field by polarizer of system ideal output as:

$$E = L_p \cdot L_{out} \cdot L_{MC} \cdot L_{45} \cdot L_{\lambda/4} \cdot L_{fout} \cdot L_m \cdot L_{fin} \cdot L_{\lambda/4} \cdot L_{MC} \cdot L_p$$

$$\boldsymbol{E} = \begin{bmatrix} \frac{E_x}{8}\left(e^{-i(2F+x-y-m)} + e^{i(2F+x-y+m)}\right) \\ 0 \end{bmatrix}$$

Expressed as the intensity of light:

$$I^* = |E|^2 = \frac{I_0}{16}\{1+\cos\{4F + 2[\varphi(t) - \varphi(t-\tau)]\}\}$$

5. Error Analysis

Define the relative error:

$$\frac{\Delta I}{I} = \frac{I_{out} - I^*_{out}}{I^*_{out}}$$

I^*_{out} is ideal output, and additional relative error is less than 0.2% was required in the ideal case.

5.1. Y Waveguide Polarizer

Definition Y waveguide polarizer pair of shaft angle θ, the ideal case is equal to 0 °. It is difficult to achieve such a precise docking in general the welding. The Y waveguide polarizer Jones matrix:

$$Lp = \begin{bmatrix} \cos^2\theta & \frac{1}{2}\sin 2\theta \\ \frac{1}{2}\sin 2\theta & \sin^2\theta \end{bmatrix}$$

Expression for the relative error to polarizer angle is:

$$I = -\frac{I_0}{8}((\sin 2\theta + 1)\cdot \sin^2 2\theta \cdot \sin^2 2F + \sin^2 2F - i\sin 2\theta \cdot \sin 4F - 1)$$

Figure 4 shows the relative error of Y waveguide polarizer pair of shaft angle, seem from Figure 4 relative error is 0.21% when θ=±0.06°, and relative error is 0.175% when θ=±0.05°. Docking of the polarizer should be in the required value within ± 0.05 ° in order to the output accuracy within 0.2%.

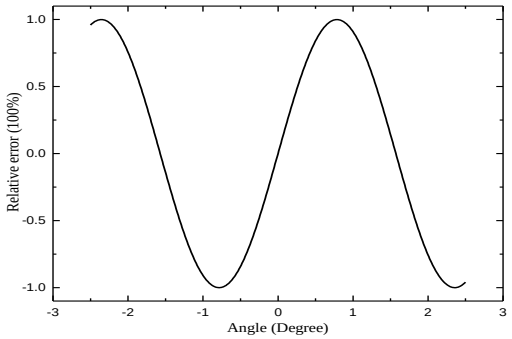

Figure 4. The Relative Error of Y Waveguide Polarizer

5.2. Sagnac Effect

The dotted line in Figure 2 equivalent to the ring interferometer, because of the two-way reciprocal interfering beams through optical paths at different times through the delay line. When Delay Sagnac effect generated by the vibrations, a measurement error was produced because of Sagnac effect and Faraday effect are the nonreciprocal effects but cannot distinguish. The definition of the two counter-propagating light beams retardation of vibrations caused by external factors is δ, and assuming the media is linear.

The Jones matrix of right-line optical compensation coil:

$$Lci\ 2 = \begin{bmatrix} \cos(\delta) & -\sin(\delta) \\ \sin(\delta) & \cos(\delta) \end{bmatrix}$$

The Jones matrix of left-line optical compensation coil:

$$Lco\ 2 = \begin{bmatrix} \cos(\delta) & \sin(\delta) \\ -\sin(\delta) & \cos(\delta) \end{bmatrix}$$

The Jones matrix of right-line optical delay coil:

$$Lci\ 1 = \begin{bmatrix} \cos(\delta) & \sin(\delta) \\ -\sin(\delta) & \cos(\delta) \end{bmatrix}$$

The Jones matrix of left-line optical delay coil:

$$Lco\ 1 = \begin{bmatrix} \cos(\ \delta\ ) & -\sin(\ \delta\ ) \\ \sin(\ \delta\ ) & \cos(\ \delta\ ) \end{bmatrix}$$

The Jones matrix of light on the right line:

$$Li\ =\ Li\,1 \cdot Li\,2$$

$$= \begin{bmatrix} \cos\ \delta & \sin\ \delta \\ -\sin\ \delta & \cos\ \delta \end{bmatrix} \begin{bmatrix} \cos\ \delta & -\sin\ \delta \\ \sin\ \delta & \cos\ \delta \end{bmatrix} = \begin{bmatrix} 1 & 0 \\ 0 & 1 \end{bmatrix}$$

The Jones matrix of light on the left line:

$$Lo\ =\ Lo\,1 \cdot Lo\,2$$

$$= \begin{bmatrix} \cos\ \delta & -\sin\ \delta \\ \sin\ \delta & \cos\ \delta \end{bmatrix} \begin{bmatrix} \cos\ \delta & \sin\ \delta \\ -\sin\ \delta & \cos\ \delta \end{bmatrix} = \begin{bmatrix} 1 & 0 \\ 0 & 1 \end{bmatrix}$$

It can to be seen form Jones matrix, vibration factors not influence of programs output equation, so it prove the feasibility of this scheme from theory.

5.3. 90°splice

Weld angle deviation is defined as α, the Jones matrix is:

$$L_{90-\alpha} = \begin{bmatrix} \sin\ \alpha & -\cos\ \alpha \\ \cos\ \alpha & \sin\ \alpha \end{bmatrix}$$

Expression for the relative error to 90°splice angle is:

$$I = \frac{I_0}{16}\{\cos^{\ 2}\alpha\,[1 + \cos(\ \phi_m \sin\ \omega_m t + 4F\ )] + \sin^{\ 2}\alpha\ \cos^{\ 2}\alpha\,(1 + \cos\ 4F\ )\}$$

Figure 5 shows the relative error of 90°splic shaft angle, seem from Figure 5 the relative error increase with the increase of the welding angle deviation, the relative error is maximum when θ=±90°, at this point no 90 ° welding and interference light signal. And relative error close to the 0 within ±10°, impact on the measurement accuracy of the system can be ignored so alignment error for welding machine 1° within the general.

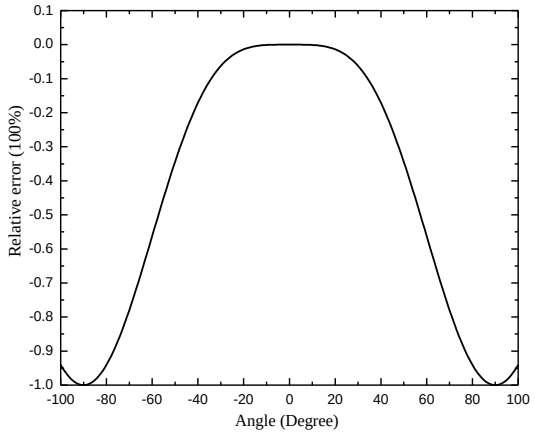

Figure 5. The Relative Error of 90° Splice

6. Conclusions

In this study, we offered a new reflective of Sagnac FOCS, a Y waveguide and external compensation coil was used to eliminate the vibration sensitivity. The key optical components in FOCS show error characteristics, including Y waveguide, Sagnac effect and 90°splice were analysis. The results provide a possible reference for further research in the FOCS techniques area.

Acknowledgements

The authors thank National Natural Science Foundation of China (51307036), Natural Science Foundation of Heilongjiang Province of China (E201303) and the Education Department of Heilongjiang province of China (12531134).

References

[1] K. T. V. Grattan and T. Sun, "Dr. Fiber optic sensor technology: an overview", Sensors and Actuators A: Physical, vol. 82, no. 1-3, **(2000)**, pp. 40-61.
[2] P. Roriz, L. Carvalho, O. Frazãob, J. Luís Santosb and J. António Simõesa, "From conventional sensors to fibre optic sensors for strain and force measurements in biomechanics applications: A review", Journal of Biomechanics, vol. 47, no. 6, **(2014)**, pp. 1251-1261.
[3] H. Zhou Yanga, X. Guang Qiaoa, D. Luoc, K. Sing Limb, W. Yi Chongb and S. Wadi Harunb, "A review of recent developed and applications of plasticfiber optic displacement sensors", Measurement, vol. 48, **(2014)**, pp. 333-345.
[4] Z. Qu, Q. Zhao and Y. Meng, "Improvement of sensitivity of eddy current sensors for nano-scale thickness measurement of Cu films", NDT & E International, vol. 61, **(2014)**, pp. 53-57.
[5] L. Yang, A. Frank, R. Wüest, B. ülenaltin, M. Lenner, G. M. Müller and K. Bohnert, "A Study on Different Types of Fiber Coils for Fiber Optic Current Sensors", Key Engineering Materials, vol. 605, **(2014)**, pp. 283-286.
[6] J. B. Roldán, C. Reig, S. Cardoso, F. Cardoso, R. Ferreira and P. P. Freitas, "An in-depth noise model for giant magnetoresistance current sensors for circuit design and complementary metal–oxide–semiconductor integration", Journal of Applied Physics, vol. 115, no. 17, **(2014)**, pp. 514-519.
[7] H. Li, C. Yang, Y. G. Hu, B. Zhao, M. Zhao and Z. Chen, "Fault-tolerant control for current sensors of doubly fed induction generators based on an improved fault detection method", Measurement, vol. 47, **(2014)**, pp. 929-937.
[8] M. Ritou, S. Garnier, B. Furet and J. Y. Hascoet, "Angular approach combined to mechanical model for tool breakage detection by eddy current sensors", Mechanical Systems and Signal Processing, vol. 44, no. 1-2, **(2014)**, pp. 211-220.
[9] F. V. B. de Nazaré, M. M. Werneck and R. P. de Oliveira, "Development of an Optical Sensor Head for Current and Temperature Measurements in Power Systems", Journal of Sensors, vol. 13, 393406:1-12, **(2013)**.
[10] H. Li, X. Cai and G. Zhang, "Transient Performances Analysis and Experiment for Optical Current Transformer", Lecture Notes in Electrical Engineering, vol. 238, **(2014)**, pp. 841-848.
[11] G. A. Sanders, "Commercialization of fiber-optic current and voltage sensors at NxtPhase", Optical Fiber Sensors Conference Technical Digest, 15th. IEEE, **(2002)**, pp. 31-34.
[12] K. Sadik and G. Karady George, "Complete Model Development for an Optical Current Transformer", IEEE Transactions on power delivery, vol. 27, no. 4, **(2012)**, pp. 1755-1762.
[13] G. Jianping, Y. Jian and Y. Hualei, "Secondary-Side Signal Processing of Fiber-Optic Current Transducer Based on LTC1068", Electronic Science and Technology, vol. 25, no. 3, **(2012)**, pp. 69-71.
[14] N. Wang and Q. Wan, "Application of the Fiber Optical Current Transformer in the 110kV Smart Substation", Asia-Pacific Power and Energy Engineering Conference (APPEEC), **(2012)**, vol. 1-4.
[15] Y. Wen-bin, L. Shen-wang and Z. Guo-qing, "Self-healing Optical Current Transformer and Its Application in Smart Substation", Electronic Information and Electrical Engineering, vol. 19, **(2012)**, pp. 340-345.
[16] J. Zubia, L. Casado and G. Aldabaldetreku, "Design and Development of a Low-Cost Optical Current Sensor", Sensors, vol. 13, **(2013)**, pp. 13584-13595.
[17] R. M. Silva, H. Martins, I. Nascimento, J. M. Baptista, A. Lobo Ribeiro, J. Santos, P. Jorge and O. Frazão, "Current Sensing Techniques- A Review", Appl. Sci., vol. 2, **(2012)**, pp. 602-628.
[18] C. Zhou, D. L. Wang, W. J. Zhang, L. Wu and Y. Yao, "Fiber Bragg grating high-current sensor based on magnetic coupling", Proc. of SPIE, 8034:1-8, **(2011)**.
[19] R. A. Bergh, H. C. Lefevre and H. J. Shaw, "An overview of fiber-optic gyroscopes", J. Lightw. Technol., vol. 2, **(1984)**, pp. 91-107.
[20] H. Lefevre, "The Fiber-Optic Gyroscope", Boston, MA: Artech House, **(1993)**.

[21] K. Bohnert, P. Gabus, J. Nehring and H. Brändle, "Temperature and vibration insensitive fiber-optic current sensor", J. Lightw. Technol., vol. 20, no. 2, **(2002)**, pp. 267-276.
[22] N. Pawel, M. W. Craig and W. Iain, "Field Evaluation of FR5 Glass Optical Current Transducer", SPIE 4074:146-154, **(2000)**.

